Available online at www.sciencedirect.com
ScienceDirect
International Journal of Solids and Structures 45 (2008) 129–143
INTERNATIONAL JOURNAL OF SOLIDS AND STRUCTURES
www.elsevier.com/locate/ijsolstr

The effect of contact on the decohesion of laminated beams with multiple microcracks

Alberto Carpinteri [a], Marco Paggi [a,*], Giorgio Zavarise [b]

[a] *Politecnico di Torino, Department of Structural and Geotechnical Engineering, Corso Duca degli Abruzzi 24, 10129 Torino, Italy*
[b] *University of Salento, Department of Innovation Engineering, Via per Monteroni – Edificio "La Stecca", 73100 Lecce, Italy*

Received 21 October 2006; received in revised form 15 June 2007
Available online 31 August 2007

Abstract

The problem of interface decohesion in laminated beams is addressed with reference to the debonding double cantilever beam test geometry (DCB). The paper deals with the analysis of the influence of nonuniform bonding properties or interfacial defects on the crack propagation process and its stability. To this aim, the classical analytical approach based on the Euler–Bernoulli beam on an elastic foundation is extended to the presence of a general distribution of microcracks ahead of the macrocrack tip. The main features and limitations of this approach are carefully analyzed. In particular, it is shown that this simplified approach does not consider the unilateral contact condition along the interface, thus admitting a penetration between the two arms of the beam. A comparison with a finite element formulation is proposed to assess if this violation of the constraints inequalities, usually adopted in the case of uniform bonding, is still acceptable when interfacial defects are present. In order to fully describe the whole nonlinear behavior of the interface, a generalized interface constitutive law is used. The models comparison shows that, in the presence of interfacial defects, the effect of contact plays a crucial role in the description of the mechanical response of the joint.

Keywords: Interfaces; Decohesion; Contact mechanics; Cohesive models; Finite elements

1. Introduction

Nowadays the problem of debonding occurring at the interface between different materials is the subject of extensive research. Most of the contributions in this field have focused on the mathematical and numerical modeling of the nonlinear mechanical response of the interface (Carpinteri et al., 2007; Paggi, 2005; Wriggers et al., 1998). In this framework, cohesive models are largely adopted to set up a local interface constitutive law. The origin of such laws can be traced back to the work of Dugdale (1960) and Barenblatt (1962), where tractions on zones near the crack tip were used to model plastic yielding in ductile materials. Extensions to the

* Corresponding author. Tel.: +39 011 564 4910; fax: +39 011 564 4899.
E-mail addresses: alberto.carpinteri@polito.it (A. Carpinteri), marco.paggi@polito.it (M. Paggi), giorgio.zavarise@unile.it (G. Zavarise).

0020-7683/$ - see front matter
doi:10.1016/j.ijsolstr.2007.07.012

analysis of the nonlinear fracture process zone in quasi-brittle materials were also proposed by Hillerborg et al. (1976), whereas Carpinteri firstly applied a cohesive formulation to the study of ductile-brittle transition and snap-back instability in concrete (Carpinteri, 1985, 1989a,b; Carpinteri and Colombo, 1989; Carpinteri et al., 1986). More recently, we have proposed an interpretation of size-scale effects in metal matrix composites and their connection with superplasticity by modeling the debonding between fibers and matrix with a cohesive formulation (Carpinteri et al., 2005).

According to this approach, the localized damaged zone can be modeled as a pair of surfaces with no volume between them. The local stress state can be replaced by an equivalent traction acting on the surfaces, which nonlinearly depends on the amount of displacement discontinuity. It has been recently demonstrated that the maximum stress that can be supported by the interface, as well as the total area under the traction-separation curve, (which is a measure of the fracture energy), are the fundamental parameters characterizing the behavior of the interface. A less important role is played by the shape of the traction-separation curve (Williams and Hadavinia, 2002). Such input parameters are usually estimated according to conventional mechanical tests designed to evaluate the properties of the interface (Cognard, 1986, 1987; Crosley and Ripling, 1991; RILEM, 1985). Among them, the debonding double cantilever beam geometry (DCB) is widely adopted for the evaluation of the Mode I fracture energy (see Fig. 1 for a scheme of the tested geometry and refer to ASTM (1993) for more details on the testing procedure).

Most of the available analytical models for the analysis of these problems in the framework of Nonlinear Fracture Mechanics are based on the theory of a beam on an elastic foundation (Massabó and Cox, 1999) and assume uniform bonding properties (Kanninen, 1973; Li et al., 2004; Qiao et al., 2003; Williams and Hadavinia, 2002). The issue of compressive stresses ahead of a macrocrack in a DCB specimen does not require a special attention when the whole beam is modeled, as for instance in Linear Elastic Fracture Mechanics. However, in the context of the theory of a beam on an elastic foundation, the actual beam geometry is simplified by considering only one half of the beam supported by elastic springs simulating the presence of interface cohesive tractions. Thus, positive and negative vertical displacements occur along the beam axis and the unilateral contact condition along the interface is not fulfilled, admitting hence an interpenetration between the two arms of the cantilever beam. This simplification is usually considered acceptable in the case of uniform bonding, since these compenetrations are thought to be recovered by the finite thickness of the adhesive. In addition, if the influence of the shear deformation is taken into account, the effect of contact is expected to be less important (Cannarozzi and Tralli, 1984). On the other hand, when multiple defects are present along the interface, traction-free portions have to be considered. In this case, the problem of enforcing the satisfaction of the unilateral contact constraint arises and is crucial (see e.g., Andrews et al., 2004 for the vibration of laminated beams with multiple cracks).

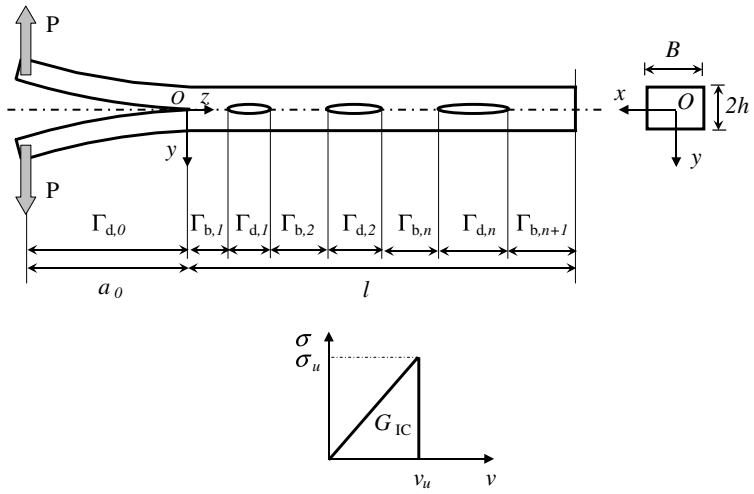

Fig. 1. Scheme of a DCB with multiple microcracks ahead of the macrocrack tip and shape of the cohesive law used for the analytical model.

Concerning the numerical models, the finite element method is usually employed with a proper discretization of the candidate contact zones with interface elements. In general, a great attention is given to the cohesive law, whereas a minor attention is provided to the contact problem, which is not explicitly addressed (Iannucci, 2006; Point and Sacco, 1996; Tenchev and Falzon, 2006). In fact, in most of the commercial FE programs, a penalty-like relation is directly added to the cohesive formulation to deal with the problem of crack closure, and only in a few cases the contact unilateral constraint is properly modeled (Ortiz and Pandolfi, 1999).

Concerning the problem of decohesion in laminated beams with interfacial defects, this study is motivated by the fact that adherend surface preparation plays a critical role in developing bonded joints. Inadequate surface roughening, environmental effects, peel ply chemical contamination, and other factors (both mechanical and chemical) can prevent adhesives from bonding properly to composites, resulting in interfacial failures and localized regions of extremely weak bonding (Bardis and Kedward, 2002). As a consequence, the mechanical response of the DCB test expressed in terms of pulling force, P, vs. crack mouth opening displacement, CMOD, results in an extremely jagged curve (see Fig. 2).

In this context, aiming at modeling such unstable mechanical responses, we extend the classical analytical approach based on the Euler–Bernoulli beam on an elastic foundation to the presence of a general distribution of microcracks ahead of the macrocrack tip. The main features and limitations of this approach are analyzed. In particular, since the contact constraint is not fulfilled with this method, a finite element model is also proposed with the aid of a generalized interface constitutive law. The advantages and the limitations of the two formulations are deeply discussed, with special emphasis to the issue of stability of crack propagation.

2. Analytical model

2.1. Mathematical formulation

Let us consider a DCB composed of two arms made of the same material and bonded along the z-axis, as schematically shown in Fig. 1. A number of debonded regions are considered along the symmetry line to model manufacturing imperfections. At this stage, we remark that no restrictions upon their distribution are made. Along the bonded portions of the beam we postulate the existence of a cohesive traction-separation law representing an elastic-perfectly brittle mechanical behavior (see Fig. 1). This relationship has been adopted by several researchers as a simplified version of a more realistic cohesive law (see e.g., Kanninen, 1973; Wriggers et al., 1998).

To determine the relationship between the critical load required for delamination, P, and the crack length, a, or equivalently the crack mouth opening displacement, CMOD, we model the upper arm of the composite

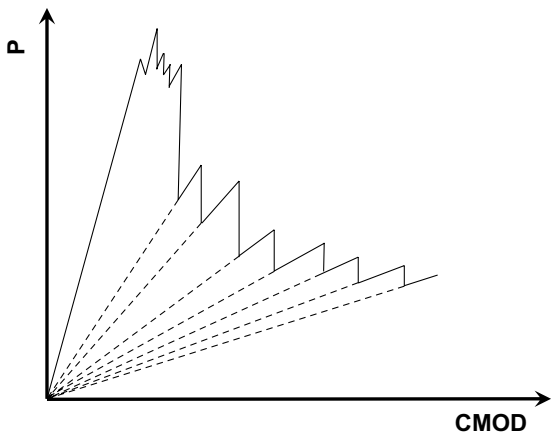

Fig. 2. A typical unstable mechanical response of a DCB test due to nonuniform bonding properties (experimental data adapted from Bardis and Kedward (2002)).

structure as an Euler–Bernoulli beam on an elastic foundation (see e.g., Williams and Hadavinia, 2002, for similar applications under the assumption of uniform bonding properties along the whole interface). This approach is widely followed in the literature and recent developments include the analysis of the effects of shear deformation (Li et al., 2004) and the study of decohesion in tapered joints with a nonconstant beam depth (Qiao et al., 2003).

In our proposed formulation, crack propagation takes place when the energy release rate equals its critical value, i.e., when $G_{\mathrm{I}} = G_{\mathrm{IC}}$, where $G_{\mathrm{IC}} = \sigma_u v_u/2$, as defined by Williams and Hadavinia (2002) and according to Fig. 1. Therefore, debonding occurs when the vertical displacement at the macrocrack tip becomes equal to v_u. This implies that, to solve the problem, the vertical displacements along the interface have to be preliminary determined.

Assuming for convenience the origin of the reference system at the macrocrack tip, two domains have to be separately discussed: the bonded domain, $\Gamma_b = \bigcup_{j=1}^{n+1} \Gamma_{b,j}$, and the debonded one, $\Gamma_d = \bigcup_{j=1}^{n} \Gamma_{d,j}$ (see Fig. 1). In this formulation the parameter n denotes the total number of defects. Neglecting the effect of shear deformation, the following fourth order ODE can be considered for the vertical displacements of the bonded portions of the beam, in agreement with the Euler–Bernoulli beam theory (Carpinteri, 1997):

$$\frac{\mathrm{d}^4 v}{\mathrm{d}z^4} = \frac{q}{\mathrm{EI}} = -\frac{B\sigma_u^2}{2\mathrm{EIG_{IC}}} v = -\frac{4}{\Delta^4} v \tag{1}$$

where the distributed load is due to the cohesive tractions multiplied by the thickness of the beam, $q = -B\sigma$, that are a linear function of the interface opening, v, as shown in Fig. 1. The parameter $\Delta = \sqrt[4]{8\mathrm{EIG_{IC}}/(B\sigma_u^2)}$ has the dimension of length and represents a characteristic parameter of the interface. The solution of this ODE is:

$$v(z) = \mathrm{e}^{-\frac{z}{\Delta}}\left(B_{4j-3}\sin\frac{z}{\Delta} + B_{4j-2}\cos\frac{z}{\Delta}\right) + \mathrm{e}^{\frac{z}{\Delta}}\left(B_{4j-1}\sin\frac{z}{\Delta} + B_{4j}\cos\frac{z}{\Delta}\right) \tag{2}$$

As usual, beam rotation, φ, bending moment, M, and shear force, T, can be simply obtained after differentiation of v (Carpinteri, 1997).

For the debonded portions of the beam, the cohesive tractions q in Eq. (1) are equal to zero and the solution of this fourth order ODE is:

$$v(z) = \frac{D_{4j-3}}{6} z^3 + \frac{D_{4j-2}}{2} z^2 + D_{4j-1} z + D_{4j} \tag{3}$$

Also in this case, beam rotation, bending moment and shear force can be obtained after differentiation.

As a result, we have $4n + 4(n+1) = 4 + 8n$ unknowns that have to be determined by imposing the boundary conditions. More specifically, four boundary conditions consist in the values of the bending moment and shear force at $z = 0$ and at $z = l$, i.e., at the macrocrack tip and at the end of the beam:

$$\begin{aligned} M(0) &= Pa_0 \\ T(0) &= P \\ M(l) &= 0 \\ T(l) &= 0 \end{aligned} \tag{4}$$

Moreover, continuity conditions of deflection, rotation, bending moment and shear force at the cross-sections between bonded and debonded beam portions have to be imposed:

$$
\begin{aligned}
&v(\overline{\Gamma}_{b,j}) = v(\overline{\Gamma}_{d,j})\\
&\varphi(\overline{\Gamma}_{b,j}) = \varphi(\overline{\Gamma}_{d,j})\\
&M(\overline{\Gamma}_{b,j}) = M(\overline{\Gamma}_{d,j})\\
&T(\overline{\Gamma}_{b,j}) = T(\overline{\Gamma}_{d,j})\\
&v(\overline{\Gamma}_{d,j}) = v(\overline{\Gamma}_{b,j+1})\\
&\varphi(\overline{\Gamma}_{d,j}) = \varphi(\overline{\Gamma}_{b,j+1})\\
&M(\overline{\Gamma}_{d,j}) = M(\overline{\Gamma}_{b,j+1})\\
&T(\overline{\Gamma}_{d,j}) = T(\overline{\Gamma}_{b,j+1})
\end{aligned}
\tag{5}
$$

where the symbol $(\overline{\cdot})$ denotes the boundary of the corresponding domains and the index j ranges from 1 to n. As a result, $4 + 8n$ equations are derived and the corresponding equation set can be symbolically written as:

$$\mathbf{K}\mathbf{x} = \mathbf{f} \tag{6}$$

where the vector $\mathbf{x}$ collects the $4 + 8n$ unknowns of the problem. The solution of this equation set provides a closed-form relationship between the unknowns in the vector $\mathbf{x}$ and the variables governing the debonding problem. Such variables are, for a given macrocrack length, the external load, the parameters of the cohesive law, as well as the distribution and the number of defects. Once the problem is solved for a trial value of the external load, the critical force for delamination can be simply determined by imposing the condition $v(z = 0) = v_u$.

This computation can be repeated by considering different macrocrack lengths ranging from a_0 to $a_0 + l_{b,1}$, where $l_{b,1}$ denotes the length of the first ligament region, $\Gamma_{b,1}$. At that point of the simulation the macrocrack tip reaches the first microcrack. Subsequent macrocrack length increments require a modification of the equation set (6) by eliminating the continuity conditions (5) corresponding to the first defect, i.e., the equations with the index $j = 1$. The same reasoning has to be repeated when the macrocrack tip reaches the subsequent microcracks.

2.2. Closed-form solution example

As a case study, let us consider a DCB test with the following geometrical and mechanical parameters: $a_0 = 30$ mm, $l = 70$ mm, $h = 1.5$ mm, $B = 1$ mm, $E = 69$ GPa, $\sigma_u = 57$ MPa, $G_{IC} = 10$ kN/m. We consider the existence of internal debonded regions, each one having a length equal to that of the bonded portions, and periodically distributed along the interface. Under these conditions, the length of the regions $\Gamma_{d,i}$ and $\Gamma_{b,i}$ is equal to $l_d = l/(2n + 1)$. Considering a number of defects, n, ranging from 0 up to 10, the load for delamination is computed as a function of the crack mouth opening displacement for crack extensions ranging from a_0 up to $a_0 + l_d$, i.e., up to reaching the first microcrack (see Fig. 3).

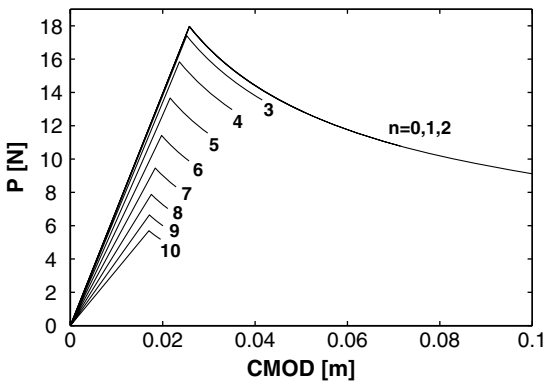

Fig. 3. Force vs. CMOD curves for a DCB test with n periodically distributed defects.

The solution of the problem (6) with the suitable boundary conditions set (4) and the continuity conditions set (5) has been obtained using MATLAB. Fig. 3 clearly shows that the peak load corresponding to the onset of delamination and the initial stiffness of the composite beam, measured as the slope of the P vs. CMOD curves before reaching the peak load, are both decreasing functions of the number of defects. Moreover, the analytical model predicts that, for the mechanical parameters herein considered, the P vs. CMOD curves corresponding to $n = 0$, 1, and 2 are almost coincident. This result can be easily interpreted by recalling the fundamental properties of the mathematical formulation of a beam on an elastic foundation. In fact, according to this model, it is well-known that, for a semi-infinite beam subjected to a concentrated force, P, and to a bending moment, $M = Pa_0$, on the left hand side, the induced vertical displacements tend to vanish for $z > \pi\Delta$. Hence, defects whose locations are beyond this distance from the macrocrack tip are expected to have a negligible effect on the behavior of the interface, as compared to the totally bonded case. For the present case study we have $\Delta = 4.7$ mm and hence $\pi\Delta = 14.7$ mm. As a consequence, since the beams with $n = 1$ and 2 have their first defect located, respectively, at $l_d = 23$ mm and at $l_d = 14$ mm from the crack tip, the corresponding crack propagation curves are similar to that for $n = 0$.

The predicted reduction in peak load and in stiffness is summarized in Fig. 4, where the ratio, R, between the peak load or stiffness and the corresponding outcomes for a beam without defects is plotted as a function of the nondimensional defect size, l_d/Δ. These nondimensional curves establish a useful one-to-one correspondence between the mechanical response of the bonded beam and the length of the periodically distributed defects placed along the interface. For instance, the peak load ratio can be evaluated from a single experimental DCB test. The corresponding nondimensional length of the defects can be determined from Fig. 4 and used to assess the quality of the bonding process. However, as it will be shown in the sequel using the finite element model, this analytical approach overestimates the degradation of the interface properties.

Finally, the results of the simulation of the whole debonding process for a DCB with $n = 3$ defects is shown in Fig. 5. The point A corresponds to the achievement of the critical condition $G_I = G_{IC}$ at the macrocrack tip for a macrocrack length equal to a_0. Points from A to B are representative of macrocrack growth from a_0 up to $a_0 + l_d$. At that point of the simulation the first bonded portion of the interface is totally debonded. Hence, a sudden reduction in the force P takes place, down to the reference curve CD which corresponds to the mechanical response of the DCB with one debonded length equal to $a_0 + 2l_d$ plus one defect. Therefore, the point D corresponds to the achievement of the critical condition $G_I = G_{IC}$ at the macrocrack tip for the new macrocrack length equal to $a_0 + 2l_d$. Exactly the same behavior is repeated when the next microcracks are encountered.

2.3. Limits and capabilities of the analytical model

As shown in the previous section, the proposed analytical model can be used to predict the vertical load vs. CMOD curve not only for DCB tests with totally bonded interfaces, but also in the presence of interfacial

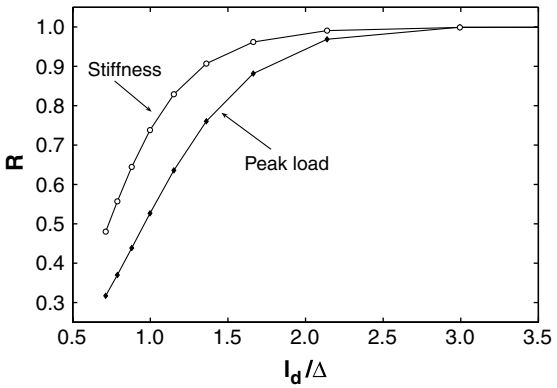

Fig. 4. Ratio between the stiffness or the peak load for a defective beam and the corresponding outcomes in case of a totally bonded interface.

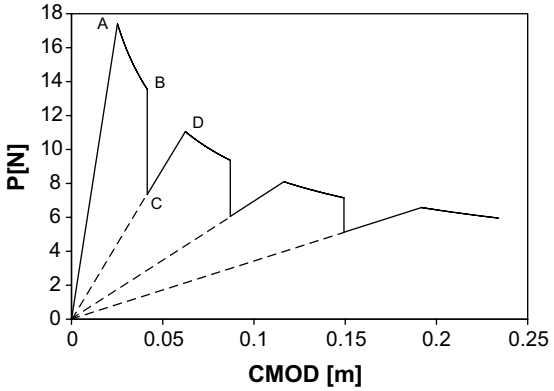

Fig. 5. Force vs. CMOD curves for a DCB test with $n = 3$ periodically distributed defects.

defects. Moreover, although the example deals with a periodically distribution of defects, no restrictions upon the size and the location of the debonding regions exist and a fully random distribution of defects can be accounted for. The cohesive parameters can also be varied along the interface and parametric analyses can be easily carried out in order to match the unstable experimental curves like the one depicted in Fig. 2. For all of these reasons, the proposed methodology is physically sound and it represents a useful extension of previous works concerning totally bonded interfaces to the more realistic case of partially bonded joints.

However, a main limitation of this approach exists and relies in the fact that interpenetration takes place along the interface since the contact inequalities are totally disregarded in this formulation. In the model, in fact, the material between the mid-plane of the DCB and the centroidal axis of an arm is modeled as a Winkler elastic foundation bonded to a rigid surface which represents the plane of symmetry. The analysis proceeds by considering a semi-infinite beam having stiffness $Bh^3/12$, supported on an elastic foundation of stiffness k, (see also the original model proposed by Kanninen (1973)). In our case the ground stiffness can be related to the slope of the cohesive traction-separation curve. The displacements of the beam for $z > 0$ are those of a classical beam on an elastic foundation, which have both negative and positive sign. As a result, when the displacements change sign, interpenetration among the beams would take place, since the contact constraints are not enforced along the interface. This situation is schematically shown in Fig. 6, where the nondimensional vertical displacement, v/v_u, is depicted as a function of the nondimensional beam length, z/Δ, for a DCB with a totally bonded interface. As a result, cohesive tractions are present in the region from the crack tip and $z/\Delta = 0.85$, as well as in the range $4 < z/\Delta < 7$. On the contrary, the displacements in the intermediate range, i.e., for $0.85 \leqslant z/\Delta \leqslant 4$, violate the unilateral contact condition which would require $v/v_u > 0$.

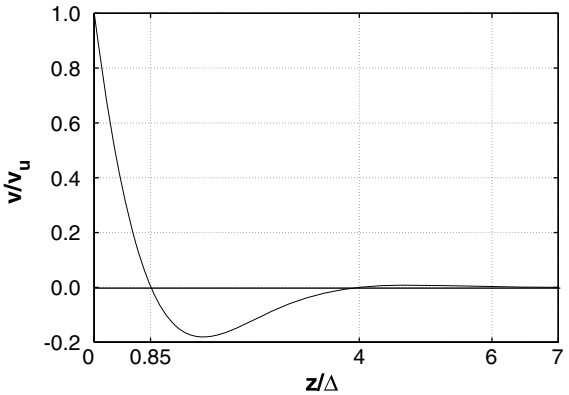

Fig. 6. Vertical displacements along the beam for a totally bonded interface according to the analytical model.

Hence, in spite of the relative simplicity of the considered problem, which is under pure Mode I deformation, a contact problem takes place due to the decohesion. This contact phenomenon, which is generally neglected when the interface is totally bonded, may have an important effect on the global response of the DCB test when multiple microcracks are present. Moreover, the occurrence of contact makes the problem highly nonlinear, since the extension of the contact area is *a priori* unknown. The use of the finite element method is then invoked to solve the problem, as shown in the next section.

3. Finite element model

3.1. Mathematical formulation

To deal with the above-described problem, interfaces are modeled according to a contact formulation which can handle cohesive forces. Contact constraints can be enforced using a modified penalty method. Depending on the contact status, an automatic switching procedure is adopted in order to choose between cohesive and contact models. According to the node-to-segment contact strategy (Wriggers, 2002), for each node along the master contact surface it is possible to compute the normal gap that is a measure of the relative displacement of the two arms of the DCB. The generalized interface constitutive law, proposed in Paggi (2005) and Paggi et al. (2006), is particularly suitable for the analysis of coupled contact and decohesion problems occurring in interface mechanical problems.

When opening takes place, interface tractions are computed according to a cohesive formulation, which is a function, respectively, of the gap measured in the normal direction, g_N, of a critical value of the opening displacement, l_{Nc}, and of the material strength, σ_u:

$$\sigma_N = \sigma_N(g_N, l_{Nc}, \sigma_u) \tag{7}$$

A linear softening cohesive law is usually adopted when the problem of cohesive crack propagation takes place inside a structural component without the presence of preexisting material discontinuities (see e.g., Carpinteri, 1989a,b; Carpinteri and Colombo, 1989; Carpinteri et al., 1986). In such a case, the cohesive tractions transmitted along the crack faces are always decreasing functions of the crack opening displacements, starting from σ_u at $g_N = 0$, down to zero when the opening is equal to the critical value, i.e., $g_N = l_{Nc}$. On the other hand, when an interface already exists, this line is usually the weakest link and the crack path is *a priori* known. In these situations the cohesive models proposed in the literature consider cohesive tractions increasing from zero up to a maximum, σ_u, in correspondence of a given interface opening, and then decreasing down to zero when $g_N = l_{Nc}$ (see e.g., the polynomial model proposed by Tvergaard (1990)). In some cases, a simplified tension cut-off relationship, like the one adopted in the derivation of the analytical model, is used to make the problem analytically treatable.

In the numerical scheme, when the inequality $g_N < l_{Nc}$ holds, the cohesive tractions computed as a function of the interface displacements are multiplied by the corresponding area of influence belonging to each Gauss point along the interface element. To do it, an enhanced formulation of the node-to-segment contact FE formulation has to be used (see Zavarise et al., 2001).

During closure, i.e., for $g_N \leqslant 0$, contact forces deriving from the interaction of the debonded interfaces can be expressed with a penalty-like model (Zavarise et al., 1992a):

$$F_N = C g_N^m \tag{8}$$

where the parameters C and m depend on the deformation assumptions of the profiles in contact. Instead of making an attempt to list the variety of approaches in the literature, we refer the reader to the survey available in Paggi et al. (2006) and Zavarise et al. (2004, 2007). Here we simply adopt a penalty formulation which is recovered by setting the penalty parameter m equal to the unity in Eq. (8).

Both in case of decohesion and contact, contributions of cohesive and contact forces are added to the global virtual work equation:

$$\delta W = \mathbb{A}(F_N \delta g_N) \tag{9}$$

where the symbol $\mathbb{A}$ denotes an assembly operator for all the interface nodes either inside the process zone or in contact.

Within the analysis, a main difficulty due to the contact constraints is related to the fact that the debonded regions are *a priori* unknown, and the corresponding boundary value problem has to be solved with an iterative method. The Newton–Raphson solution procedures, commonly used for solving nonlinear problems, require the determination of the tangent stiffness matrix. Consistent linearization of the equation set (9) leads to:

$$\Delta\delta W = \frac{\partial F_N}{\partial g_N}\Delta g_N \delta g_N + F_N \Delta\delta g_N \tag{10}$$

where symbols δ and Δ denote, respectively, variations and linearizations. In Eq. (10) the normal forces are given by either the cohesive formulation, or the contact model. Linearizations and variations of the normal gap can be found in Zavarise et al. (1992b) for the contact model and in Paggi (2005) for the cohesive law, as well as the discretized version of these expressions for a direct implementation in the finite element formulation.

3.2. Interface discretization

Interfaces can be properly modeled in the finite element framework as contact surfaces with the virtual node technique (Zavarise et al., 2001). The basic idea underlying this method consists in changing the integration scheme usually adopted for the node-to-segment contact elements. In this formulation the cohesive/contact contribution to the stiffness matrix and the internal force vector are integrated on the contact element through a n-point Gauss integration scheme. In this context, the classical node-to-segment scheme can be seen as a 2-point Newton–Cotes integration one. In this way, an arbitrary number of Gauss points can be specified inside each contact element placed along the interface, regardless of the discretization used for the continuum. This method permits to achieve a fine discretization of the interface, where the interfacial constitutive laws exhibit a strong nonlinearity, without refining the discretization of the continuum.

To show the effectiveness of this method, an example of decohesion between two bonded rectangular blocks is illustrated. The adhesive zone is 2 m long and the Young's moduli of the two materials are equal to 1000 Pa, whereas the Poisson's ratios are equal to 0.3. A coarse mesh is used for the discretization of the continuum in the horizontal direction. During the simulation, vertical displacements with a linear variation along the horizontal direction from zero to $v_{\max}$ are imposed to the bottom side of the lower block (see the deformed mesh depicted in Fig. 7).

Debonding is modeled according to a polynomial nonlinear cohesive model (Tvergaard, 1990). The critical normal separation, l_{Nc}, and the peak value of the cohesive traction, σ_u, are assumed equal to 0.2 μm and 30 Pa, respectively. Starting from the left side and denoting with x the distance along the interface, the variation of the normal gap measured at the Gauss points, g_N, is depicted as a function of x in Fig. 8a. Due to the displacement field interpolation, the expected linear variation is achieved, regardless of the number of Gauss points

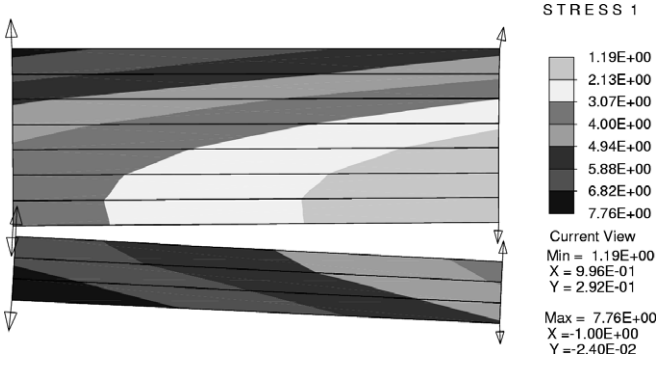

Fig. 7. Deformed mesh of the test problem.

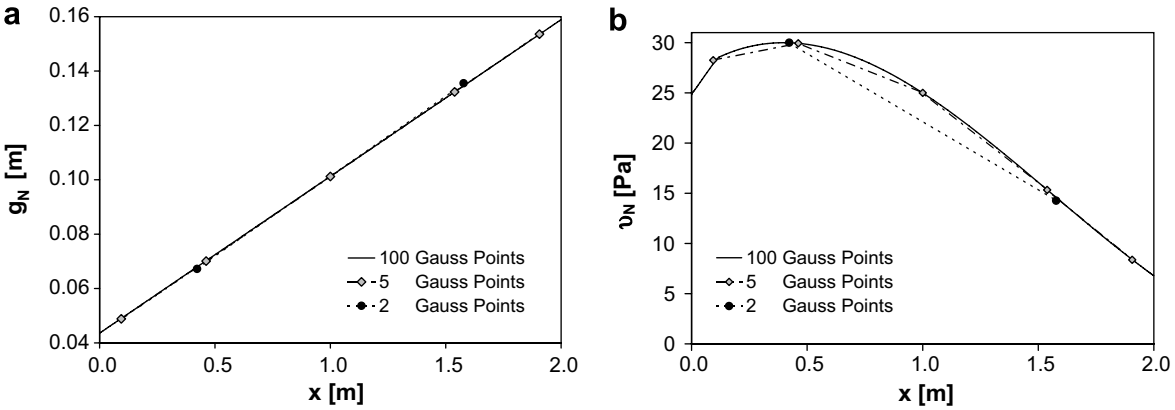

Fig. 8. (a) Normal gap, g_N, and (b) cohesive tractions, σ_N, computed at Gauss points along the interface for different interface discretizations characterized by 2, 5, and 100 Gauss points.

considered in the model. On the other hand, a completely different trend is obtained for the normal cohesive tractions (see Fig. 8b). In fact, due to the nonlinearity of the interface constitutive law, the mechanical response is significantly influenced by the discretization adopted for the interface. This is particularly evident in the interface region characterized by small relative vertical displacements, where the cohesive zone-model exhibits a strong nonlinearity (see Fig. 8b in the range $0 < x < 1$). For all of these reasons, this proposed discretization technique is very well suited for the DCB test geometry, where the problem of mesh dependence occurs until when the element size is small enough to correctly reproduce the interlaminar stresses (Corigliano and Ricci, 2001).

For the proposed examples concerning defective beams with n defects, the geometrical discretization based on the node-to-segment strategy is adopted, introducing the master–slave contact segments. Such segments are simple lines in the proposed two-dimensional model. This technique allows an arbitrary sliding of a node of a slave segment over the entire master segment, which is not usually permitted with interface elements in this context (see Wriggers and Zavarise, 2004 for further details). Moreover, by subdividing the whole interface into $2n + 1$ contact segments, it is possible to specify different parameters of the interface constitutive law for each segment. In this way, the defects are simply treated by setting equal to zero the cohesive forces during interface opening.

3.3. Numerical examples

The application of our generalized interface constitutive law implemented in the finite element code FEAP (courtesy of Prof. Taylor) permits to analyze the decohesion problem taking into account the whole nonlinear interface behavior. This fact is very well evidenced in Fig. 9, where the deformed meshes for the DCB test with and without taking into consideration the contact constraints are compared. Clearly, when contact is disregarded, interpenetration of the two arms of the beam takes place, which is a physically unacceptable situation.

Fig. 10 shows a comparison between the finite element results in the case of a totally bonded interface (the input data are those of the beam previously analyzed according to the analytical model). The finite element solutions take into account the effect of contact along the interface and consider three different cohesive laws: the tension cut-off relationship between cohesive tractions and opening displacements, which has been used in the analytical model, a linear softening law (Carpinteri, 1989a,b; Carpinteri and Colombo, 1989; Carpinteri et al., 1986), and a polynomial relationship (Tvergaard, 1990). The cohesive parameters σ_u and G_{IC} are the same for all the models. The good agreement between the computed P vs. CMOD curves obtained using the three cohesive models demonstrates that the shape of the cohesive law does not play a major role.

The comparison between the outcome of the analytical model and the finite element solutions is also proposed in Fig. 10. The analytical method yields stiffer results as compared to the finite element solutions due to fact that it completely disregards the enforcement of the unilateral contact constraints along the interface. In

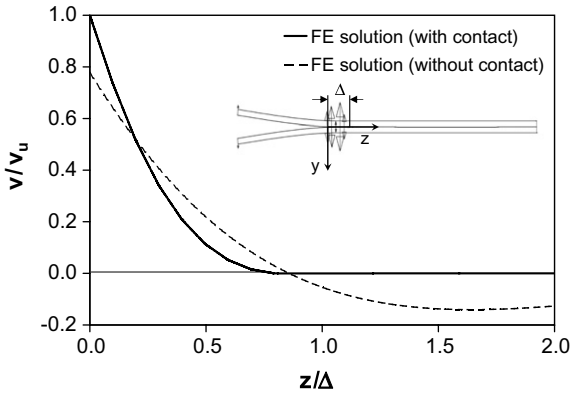

Fig. 9. Transverse displacements in the process zone for the DCB tests with or without modeling the contact constraints. Reaction forces are marked with arrows. $z = 0$ denotes the position of the macrocrack tip.

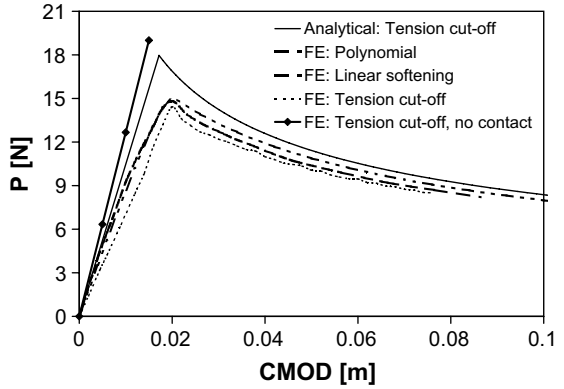

Fig. 10. Comparison between analytical and finite element solutions for a DCB test with totally bonded interface.

fact, when the problem of contact is taken into account, the transverse displacement at the macrocrack tip is increased for a given applied pulling force, P. As a consequence, the critical load for delamination becomes lower than that analytically provided and a higher compliance is observed (see Fig. 9). On the other hand, if the compenetration of the two arms of the beam is allowed in the finite element solution, by retaining only the cohesive relationship in the interface constitutive law, then we expect to obtain an approximation of the analytical solution (see the curve with square dots in Fig. 10). In this case, since the problem is discretized with a finite number of degrees of freedom, the numerical approximation turns out to be stiffer than the analytical one.

The finite element results for a DCB test with $n = 5$ and 10 defects are shown in Fig. 11. As already pointed out for the results obtained from the application of the analytical model, the peak load corresponding to the onset of delamination and the initial stiffness of the composite beam are both decreasing functions of the number of defects. Also in this case, the initial stiffness of the composite is measured as the slope of the load vs. CMOD curve before reaching the peak load. However, the expected large reduction in peak load and in stiffness predicted by the analytical model is diminished when the contact condition is taken into account. In fact, although the number of defects is increased from 5 to 10, most of them fall into a compressed zone (whose extension is approximately equal to $0.85 < z/\Delta < 4$, as expected from Fig. 6) and do not contribute to the stiffness reduction. More precisely, for the proposed example with $n = 5$, we have $l_d/\Delta = 1.36$, i.e., the first defect is entirely inside the compressed zone. Similarly, for $n = 10$, we have $l_d/\Delta = 0.72$, i.e., only a small part of the first defect ($0.72 < l_d/\Delta < 0.85$) is outside the compressed zone. As a result, the overall mechanical response is similar in the two cases.

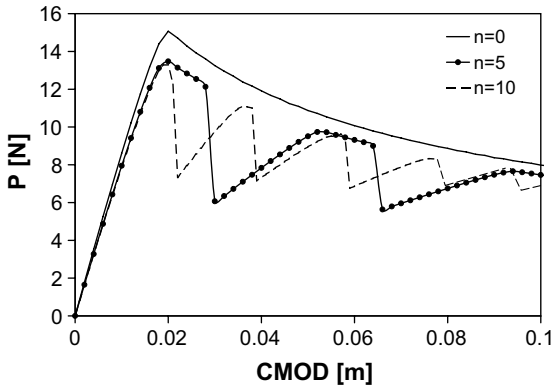

Fig. 11. Force vs. CMOD curves for a DCB test with interfacial defects: finite element solution.

Transverse stresses in the region close to the crack tip are also shown in Fig. 12, indicating the presence of compressive stresses due to contact.

Finally, it has to be pointed out that the finite element algorithm permits to follow the whole delamination process. Under displacement control, when the first bonded portion of the interface fails, a sudden reduction in the reaction force, P, takes place in response to the microcrack, when a jump in the macrocrack length occurs from $a_0 + l_d$ to $a_0 + 2l_d$ (see points A and B in Fig. 13). After that, another bonded portion of the beam is involved and the reaction force progressively increases (see points B and C in Fig. 13). The same curve BC could be followed in case of a DCB with initial crack length equal to $a_0 + 2l_d$ (see the dashed line connecting the origin of the plane with the point B in Fig. 13). Exactly the same behavior is repeated when the other defects are encountered.

The jumps in the reaction force, caused by a discrete crack advancement through the defected zone, are a typical example of crack growth instability as those found by Carpinteri and Monetto (1999) in case of fracture evolution in multi-cracked solids. As firstly noted by Carpinteri (1999), it is interesting to point out that the case of a macrocrack with a regular distribution of discrete microcracks ahead of its tip (Fig. 14a) is

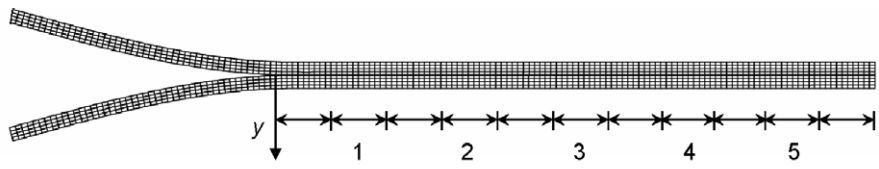

(a) Deformed mesh.

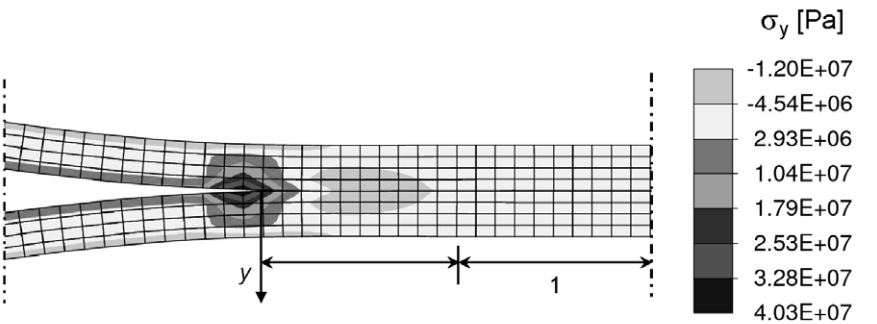

(b) Transverse stresses.

Fig. 12. Deformed mesh and contour plot of the transverse stresses in the region close to the macrocrack tip.

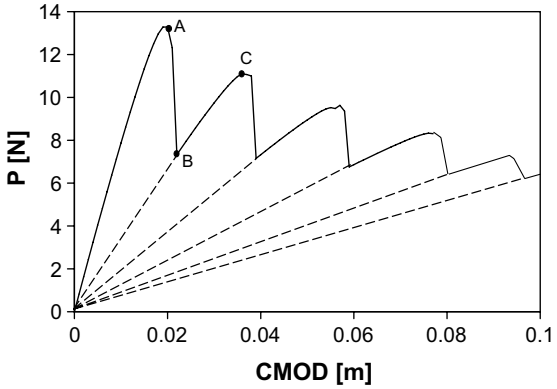

Fig. 13. Force vs. CMOD curve for a DCB test with $n = 10$ defects: detail of the unstable response.

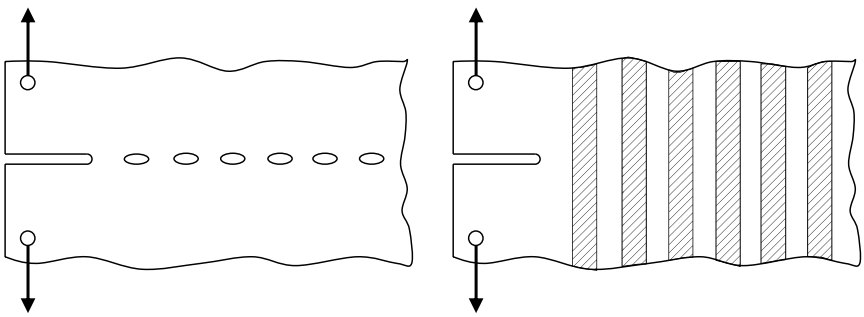

(a) Microcracked zone. (b) Reinforced zone.

Fig. 14. Analogy between microcracked and reinforced zones ahead of a macrocrack tip.

analogous to that of a macrocrack with a regular distribution of discrete reinforcements (Fig. 14b) (Carpinteri and Massabò, 1996). In both cases the structural response presents a discrete number of instabilities with related peaks and valleys. For the microcracked process zone, the valleys represent the stage of approach of the macrocrack tip to a microcrack tip. In this situation the stress state is particularly high and therefore a lower load is adequate to produce $G_I = G_{IC}$. On the other hand, the peaks represent the stage subsequent to the macrocrack–microcrack coalescence, when the new macrocrack tip is still far from the next microcrack tip. Thus its stress concentration is still relatively low. In this latter case, a higher load is needed to have $G_I = G_{IC}$ at the driving tip. The analogy between reinforced zone and microcracked zone consists therefore in a multiple irregular mechanical response, where the valleys and the peaks represent, respectively, the crack arrest at the fibers or the crack-slip coalescence, and the fiber crossing or the crack growth after coalescence.

4. Conclusion

In this contribution the problem of interface decohesion of laminated beams with nonuniform interface properties has been addressed. To this aim, an analytical model has been proposed for the analysis of decohesion in laminated beams with a generic number of microcracks randomly placed along the interface. Focusing our attention to the case of periodically distributed defects, it has been shown that the analytical model would suggest a significant reduction in peak load and stiffness when the defects are close to the crack tip, thus influencing the distribution of the cohesive tractions.

However, a careful analysis of the mechanical response provided by this model shows that its solution violates the unilateral contact conditions along the interface. This fact poses some limitations to the applicability of the foundation model to the problem of decohesion with multiple defects. The implementation of a

generalized interface constitutive law in the finite element framework permits to overcome such drawbacks and to model the whole nonlinear behavior of the interface, with particular attention to the contact problem. Moreover, cohesive laws more realistic than the tension cut-off relation can be easily considered.

The numerical results show that, in case of a totally bonded interface, the analytical approach and the numerical model are in reasonable agreement, whereas in presence of multiple defects the analytical approach significantly underestimates the value of the critical load corresponding to delamination.

Acknowledgements

The financial support provided by the Italian Ministry of University and Research to the project "PRIN2005—Modelling and approximation in advanced mechanical problems", and by the European Union to the Leonardo da Vinci projects "Numerical based medium level training on industrial friction problem (NUFRIC)" and "Innovative Learning and Training on Fracture (ILTOF)" is gratefully acknowledged.

References

Andrews, M., Massabó, R., Cox, B., 2004. Elastic interaction of multiple delaminations in laminated structures. In: Proceedings of XXI International Congress of Theoretical and Applied Mechanics ICTAM, Warsaw, Poland.

ASTM, 1993. Standard test method for fracture strength in cleavage of adhesives in bonded joints. Tech. Rep. D3433-93, American Society for Testing and Materials.

Bardis, J., Kedward, K., 2002. Surface preparation effects on Mode I testing of adhesively bonded composite joints. Journal of Composites Technology and Research 24, 30–37.

Barenblatt, G., 1962. The mathematical theory of equilibrium cracks in brittle fracture. In: Dryden, H., Karman, T.V. (Eds.), Advances in Applied Mechanics, vol. VII. Academic Press, New York, pp. 55–129.

Cannarozzi, A., Tralli, A., 1984. On the analysis of unilaterally supported plates by finite element models. International Journal of Solids and Structures 20, 179–189.

Carpinteri, A., 1985. Interpretation of the Griffith instability as a bifurcation of the global equilibrium. In: Shah, S. (Ed.), Application of Fracture Mechanics to Cementitious Composites (Proceedings of a NATO Advanced Research Workshop, Evanston, USA, 1984). Martinus Nijhoff Publishers, Dordrecht, pp. 287–316.

Carpinteri, A., 1989a. Cusp catastrophe interpretation of fracture instability. Journal of the Mechanics and Physics of Solids 37, 567–582.

Carpinteri, A., 1989b. Softening and snap-back instability in cohesive solids. International Journal for Numerical Methods in Engineering 28, 1521–1537.

Carpinteri, A., 1997. Structural Mechanics: a Unified Approach. Chapman & Hall, London.

Carpinteri, A. (Ed.), 1999. Nonlinear Crack Models for Nonmetallic Materials. Kluwer Academic Publisher, Dordrecht.

Carpinteri, A., Colombo, G., 1989. Numerical analysis of catastrophic softening behaviour (snap-back instability). Computers & Structures 31, 607–636.

Carpinteri, A., Lacidogna, G., Paggi, M., 2007. Acoustic emission monitoring and numerical Modeling of FRP delamination in RC beams with non-rectangular cross-section. RILEM Materials & Structures 40, 553–566.

Carpinteri, A., Massabò, R., 1996. Bridged versus cohesive crack in the flexural behaviour of brittle-matrix composites. International Journal of Fracture 81, 125–145.

Carpinteri, A., Monetto, I., 1999. Snap-back analysis of fracture evolution in multi-cracked solids using boundary element method. International Journal of Fracture 98, 225–241.

Carpinteri, A., Paggi, M., Zavarise, G., 2005. Snap-back instability in micro-structured composites and its connection with superplasticity. Strength, Fracture and Complexity 3, 61–72.

Carpinteri, A., Di Tommaso, A., Fanelli, M., 1986. Influence of material parameters and geometry on cohesive crack propagation. In: Wittmann, F. (Ed.), Fracture Toughness and Fracture Energy of Concrete (Proceedings of an International Conference on Fracture Mechanics of Concrete, Lausanne, Switzerland, 1985). Elsevier, Amsterdam, pp. 117–135.

Cognard, J., 1986. The mechanics of the wedge test. Journal of Adhesion 20, 1–13.

Cognard, J., 1987. Quantitative measurement of the energy of fracture of an adhesive joint using the wedge test. Journal of Adhesion 22, 97–108.

Corigliano, A., Ricci, M., 2001. Rate-dependent interface models: formulation and numerical applications. International Journal of Solids and Structures 38, 547–576.

Crosley, P., Ripling, E., 1991. A thick adherend, instrumented double-cantilever-beam specimen for measuring debonding of adhesive joints. Journal of Testing and Evaluation 19, 24–28.

Dugdale, D., 1960. Yielding in steel sheets containing slits. Journal of the Mechanics and Physics of Solids 8, 100–104.

Hillerborg, A., Modeer, M., Petersson, P., 1976. Analysis of crack formation and crack growth in concrete by means of fracture mechanics and finite elements. Cement and Concrete Research 6, 773–782.

Iannucci, L., 2006. Dynamic delamination modelling using interface elements. Computers & Structures 84, 1029–1048.

Kanninen, M., 1973. An augmented double cantilever beam model for studying crack propagation and arrest. International Journal of Fracture 9, 83–92.

Li, S., Wang, J., Thouless, M., 2004. The effects of shear on delamination in layered materials. Journal of the Mechanics and Physics of Solids 52, 193–214.

Massabó, R., Cox, B., 1999. Concepts for bridged Mode II delamination cracks. Journal of the Mechanics and Physics of Solids 47, 1265–1300.

Ortiz, M., Pandolfi, A., 1999. Finite-deformation irreversible cohesive elements for three-dimensional crack propagation analysis. International Journal for Numerical Methods in Engineering 44, 1267–1282.

Paggi, M., 2005. Interface Mechanical Problems in Heterogeneous Materials. Ph.D. thesis, Politecnico di Torino, Torino, Italy.

Paggi, M. Carpinteri, A. Zavarise, G., 2006. A unified interface constitutive law for the study of fracture and contact problems in heterogeneous materials. In: Wriggers, P., Nackenhorst, U. (Eds.), Analysis and simulation of contact problems, Lecture Notes in Applied and Computational Mechanics, vol. 27. Springer-Verlag, Berlin, pp. 297–304.

Point, N., Sacco, E., 1996. Delamination of beams: an application to DCB specimen. International Journal of Fracture 79, 225–247.

Qiao, P., Wang, J., Davalos, J., 2003. Analysis of tapered ENF specimen and characterization of bonded interface fracture under Mode-II loading. International Journal of Solids and Structures 40, 1865–1884.

RILEM, 1985. Determination of the fracture energy of mortar and concrete by means of three-point bend tests on notched beams. TC 50 Technical Committee on Fracture Mechanics of Concrete, Draft Recommendation, Materials & Structures, vol. 18, pp. 285–290.

Tenchev, R., Falzon, B., 2006. A pseudo-transient solution strategy for the analysis of delamination by means of interface elements. Finite Elements in Analysis and Design 42, 698–708.

Tvergaard, V., 1990. Effect of fiber debonding in a whisker-reinforced metal. Material Science and Engineering A 107, 23–40.

Williams, J., Hadavinia, H., 2002. Analytical solutions for cohesive zone models. Journal of the Mechanics and Physics of Solids 50, 809–825.

Wriggers, P., 2002. Computational Contact Mechanics. John Wiley & Sons, Ltd., The Atrium, Southern Gate, Chichester, West Sussex, PO19 8SQ, England.

Wriggers, P., Zavarise, G., 2004. Computational contact mechanics, encyclopedia of computational mechanics. In: Stein, E., De Borst, R., Huges, T.J.R. (Eds.), Solids and Structures, vol. 2. Springer, Chichester, pp. 195–226.

Wriggers, P., Zavarise, G., Zohdi, T., 1998. A computational study of interfacial debonding damage in fibrous composite materials. Computational Materials Science 12, 29–56.

Zavarise, G., Borri-Brunetto, M., Paggi, M., 2004. On the reliability of microscopical contact models. Wear 257, 229–245.

Zavarise, G., Borri-Brunetto, M., Paggi, M., 2007. On the resolution dependence of micromechanical contact models. Wear 262, 42–54.

Zavarise, G., Boso, D., Schrefler, B., 2001. A contact formulation for electrical and mechanical resistance. In: Proceedings of CMIS, III Contact Mechanics International Symposium, Praja de Consolacao, Portugal. pp. 211–218.

Zavarise, G., Schrefler, B., Wriggers, P., 1992a. Consistent formulation for thermomechanical contact based on microscopic interface laws. In: Owen, D., Oñate, E., Hinton, E. (Eds.), Proc. COMPLASS III, Int. Conf. on Comput. Plasticity. Springer, USA, pp. 349–360.

Zavarise, G., Wriggers, P., Stein, E., Schrefler, B., 1992b. Real contact mechanisms and finite element formulation—a coupled thermomechanical approach. International Journal for Numerical Methods in Engineering 35, 767–785.